Density-functional approach to phase transitions of submonolayer films. I. The role of the intrinsic and extrinsic ordering forces

L. Mederos, P. Tarazona, and G. Navascués
Instituto de Física del Estado Sólido and Departamento de Física del Estado Sólido, Universidad Autónoma de Madrid, Cantoblanco, 28049-Madrid, Spain
(Received 9 June 1986)

A density-functional theory for the submonolayer adsorbed film is developed. The adsorbate interactions are restricted to hard repulsions and described with a nonlocal density functional for the free energy, which allows for the presence of intrinsic crystalline order. The competition with the substrate ordering is studied as a function of the temperature and the coverage for different values of the substrate lattice parameter. The phase diagrams obtained include fluid, commensurate, and incommensurate phases.

I. INTRODUCTION

The submonolayer regime of physisorbed films exhibits quite interesting phase diagrams which include fluid condensations, order-disorder transitions, and commensurate-incommensurate (CI) transitions. This richness of transitions is due to the presence of different competing forces: the ideal entropy tending towards disorder, the hard-core interactions between adsorbate molecules trying to pack themselves in an intrinsic ordered structure, the substrate external potential inducing external ordering over the adsorbate, i.e., making the adsorbate structure commensurate with the symmetry of the substrate potential, and finally, the attractive forces between adsorbate molecules responsible for the gas-liquid condensation.

In the limit of dilute adsorbate on strongly structured substrates, the particle distribution of the adsorbate molecules $\rho(\mathbf{r})$ will have the periodicity of the substrate potential, corresponding to a fluid modulated by an external field. On the other hand a densely packed adsorbate on a weakly structured substrate may crystallize, taking on its own intrinsic periodicity independent of the substrate and, in general, incommensurate with it. In between these two limits and depending on the relative size and shape of both competing lattices, the system may find a compromise, where $\rho(\mathbf{r})$ has not the full symmetry of the substrate but only that of a sublattice, which happens to be close to the intrinsic ordering, so that by a small deformation of the intrinsic lattice the system locates each particle around a potential well of the substrate.

All these phases and the transitions between them have been studied theoretically,[1-5] experimentally,[6] and with computer simulations.[7] From the theoretical point of view, lattice models have been extensively used, e.g., the hard-hexagons model[8] provides a beautiful and exactly soluble model for the transition between the "fluid," when all the lattice sites have the same occupancy, and the "commensurate" phase when one sublattice is preferred to the other. However, despite the interest of the various lattice models, there are important points which require a continuous description of the particle distribution so that they are beyond the capability of the discrete variables used in lattice models. One of these points is the study of the modulation caused in the density distribution of the adsorbate molecules due to the interaction with the substrate. In this case one is interested in how strong the structure is, rather than what the periodicity is, so that a continuous description of $\rho(\mathbf{r})$ is required. An even more important case is the competition between the substrate order and the different and fully incommensurate intrinsic ordering. A lattice model may analyze how the tendency of the substrate to impose its periodicity is frustrated by the adsorbate-adsorbate interactions which induce a completely packed set of dislocations, but will never give rise to a completely different ordering intrinsic to the adsorbate.

Density-functional theory provides a useful framework for a continuous description of $\rho(\mathbf{r})$, for one can develop successively more refined density-functional models, which will include more aspects of the problem, giving in this way a good idea of their relative importance. This technique has been applied before to describe the "fluid" behavior and the transition to a commensurate phase. Here we present the first density-functional calculation which includes a description of the intrinsic ordering. For it we use a two-dimensional hard-disk system, which models the hard-core interaction of the adsorbate molecules, under the effect of an external field which models the noble-gas—graphite interactions. This model cannot describe the real-noble gas—graphite system because attractive interactions would need to be supplied. However it has all the ingredients necessary to determine the possible order-disorder and CI transitions, and the presence of the attractive forces would increase the stability of the different phases beside introducing the fluid condensation. This results in a quantitative change of the transition strength which can even be suppressed when they are weak enough, but adsorbate forces cannot induce any transitions other than the fluid condensation; therefore our hard-core model provides the basic structure of the phase diagram and we shall discuss it in detail before introducing attractive adsorbate interactions. This discussion does not include the effects of vacancies, interstitials and domains which, like the attractive forces, are not re-

sponsible for either the order-disorder or the CI transitions, though they will modify their strength. These effects are analyzed in the second part of this work.

The article is organized as follows. In Sec. II we propose a nonlocal density functional for the Helmholtz free energy of a hard-disk system in an external field. In Sec. III we choose the external potential which models the noble-gas—graphite interactions.[9] We also show the possible C phases which can exist of the physical density range. In Sec. IV we introduce the parametrized density as a superposition of Gaussians. This is a much better way for describing strong structured densities than a few terms of a Fourier expansion; it also describes homogeneous densities in the limit where the Gaussians have infinite width. The Gaussian width is the parameter with respect to which we minimize the Helmholtz free energy. This is done in Sec. V, where the free energy versus mean density (hereafter called a free-energy branch) for fluid, C and I phases are shown. In Sec. VI we obtain and discuss the final phase diagram from the free-energy branches and with the help of the common-tangent method. The discussion includes the evolution of the phase diagram with the substrate lattice constant in hard-disk-diameter units. This shows all possible configurations for the phase diagram. Finally, in Sec. VII we review the results and propose the necessary relaxation mechanisms which determine the final quantitative form of the phase diagram. This is done in a second part of this work.

II. A FREE-ENERGY DENSITY FUNCTIONAL FOR HARD DISKS

Nonlocal corrections[10] to local density functionals for the free energy give a poor description of strongly structured systems. For these systems a new approach has been devised where a simple nonlocal density functional is proposed and solved self-consistently.[11–13] The nonlocality of the free-energy functional is introduced through a smoothed density $\bar{\rho}(\mathbf{r})$ which is a nonlocal functional of the local density $\rho(\mathbf{r})$. $\bar{\rho}(\mathbf{r})$ is related in some way to the average of $\rho(\mathbf{r})$ over the interaction range. Following this approach, the Helmholtz free-energy functional we take is

$$F[\rho]=F_{id}[\rho]+\int d\mathbf{r}\rho(\mathbf{r})\Delta\psi[\bar{\rho}(\mathbf{r})] , \tag{1}$$

where

$$\begin{aligned}F_{id}[\rho]&=k_BT\int d\mathbf{r}\rho(\mathbf{r})\psi_{id}[\rho(\mathbf{r})]\\&=k_BT\int d\mathbf{r}\rho(\mathbf{r})\{\ln[\Lambda^2\rho(\mathbf{r})]-1\}\end{aligned} \tag{2}$$

is the ideal contribution to the free energy which is exactly local, $\Lambda^2=h^2/2\pi mk_BT$ and

$$\Delta\psi(\rho)\equiv\psi(\rho)-\psi_{id}(\rho) \tag{3}$$

is the excess with respect to the ideal case of the Helmholtz free-energy density at mean density ρ. From the Gibbs adsorption equation and the scale-particle pressure,[14]

$$p=k_BT\rho/(1-\eta)^2 , \tag{4}$$

we get for the homogeneous hard-disk fluid

$$\Delta\psi=k_BT\left[\frac{\eta}{1-\eta}-\ln(1-\eta)\right] , \tag{5}$$

where $\eta\equiv\rho d^2\pi/4$ is the packing fraction and d is the hard-disk diameter. Any other more sophisticated state equation could be chosen, but the scale-particle one is accurate enough for our purposes and it has the advantage of its simplicity. To complete the prescription of our functional we need a criterion to determine $\bar{\rho}(\mathbf{r})$. We use the expression

$$\bar{\rho}(\mathbf{r})=\int d\mathbf{r}'\rho(\mathbf{r}')\omega(|\mathbf{r}-\mathbf{r}'|) , \tag{6}$$

which defines $\bar{\rho}$ as a nonlocal functional of the local density ρ weighted by the function $\omega(r)$. In order to simplify the calculations we take the simplest choice for ω:

$$\omega(|\mathbf{r}-\mathbf{r}'|)=\begin{cases}1/\pi d^2 , & |\mathbf{r}-\mathbf{r}'|\le d\\ 0 , & |\mathbf{r}-\mathbf{r}'|>d\end{cases} \tag{7}$$

which averages the local density over a circle of radius d around $\mathbf{r}$. It has been shown[15] that the present choice corresponds to the zero-order term in the density expansion of $\omega(r;\rho)$.

The direct correlation function of the hard-disk fluid can be obtained using the functional (1):[16]

$$c(\mathbf{r},\mathbf{r}')=-\frac{1}{k_BT}\frac{\delta^2(F[\rho]-F_{id}[\rho])}{\delta\rho(\mathbf{r})\delta\rho(\mathbf{r}')} , \tag{8}$$

which, with approximation (7), gives for the homogeneous case at mean density ρ:

$$\begin{aligned}k_BTc(|\mathbf{r}-\mathbf{r}'|)=&-2\Delta\psi'(\rho)\omega(|\mathbf{r}-\mathbf{r}'|)\\&-\rho\Delta\psi''(\rho)\\&\times\int d\mathbf{r}''\omega(|\mathbf{r}-\mathbf{r}''|)\omega(|\mathbf{r}''-\mathbf{r}'|) .\end{aligned} \tag{9}$$

Approximation (7) overestimates the direct correlation function, but this still changes properly with the density and that is the important property for the aims pursued here. This approach with approximation (7) gives quite reasonable results for highly inhomogeneous systems such as hard spheres near a hard wall[16] and the melting[13] of hard spheres and hard disks; therefore we expect to have a good description of the features of the phase diagram we are interested in.

For completeness and later reference we write down the Helmholtz free-energy density and the chemical potential of an homogeneous hard-disk fluid which can be straightforwardly obtained from (5):

$$f(\rho)=k_BT\rho\left[\ln(\Lambda^2\rho)-1+\frac{\eta}{1-\eta}-ln(1-\eta)\right] \tag{10}$$

and

$$\mu(\rho)=\frac{\partial f(\rho)}{\partial\rho}=k_BT\left[\ln(\Lambda^2\rho)-\ln(1-\eta)+\frac{\eta(3-2\eta)}{(1-\eta)^2}\right] . \tag{11}$$

Observe that (10) can be obtained directly from the functional (1) showing the thermodynamic consistence of the functional approach.

In the Appendix we show the expression of the density expansion of our free-energy functional using the weight function (7). We also show the Fourier transform of this expansion. These expressions will be used later.

III. THE SUBSTRATE POTENTIAL

To complete the model we specify the interaction, $V_{\text{ext}}(\mathbf{r})$, between the adsorbate (hard disks) and the substrate and we add the corresponding extrinsic contribution to our free energy functional. We restrict ourselves to the usual periodic substrates, then

$$V_{\text{ext}}(\mathbf{r})=\sum_{\mathbf{G}_s} V_{\mathbf{G}_s}(Z)e^{i\mathbf{G}_s\cdot\mathbf{r}} , \tag{12}$$

where Z is the direction normal to the surface, $\mathbf{G}_s$ are the substrate reciprocal-lattice vectors.

Usually the substrate potential is well described by the star configuration set up by the smallest reciprocal vectors. In addition, the adsorbate is practically localized at Z_0, corresponding to the minimum of $V_{\mathbf{G}_s}(Z)$, $\mathbf{G}_s$ being any one of the mentioned star vectors; then

$$V_{\text{ext}}(\mathbf{r})=V(Z_0)\sum_{\mathbf{G}_s}{}^{*} e^{i\mathbf{G}_s\cdot\mathbf{r}} , \tag{13}$$

where $\sum^{*}$ means the sum is restricted to the first star of the lattice reciprocal vectors. Expression (13) will complete our interaction model which, for a triangular lattice, describes noble gases on graphite.[9] The model would describe real noble-gas–graphite systems if adsorbate attractive forces were included; these forces would induce the fluid condensation and most probably would modify the strength of the order-disorder and CI transitions. However these can only exist as a result of the competition of all the forces of our interaction model. The discussion of this competition will be the core of this article.

If the adsorbate has a perfect periodic structure, we can write its density distribution as

$$\rho(\mathbf{r})=\sum_{\mathbf{G}_a}\rho_{\mathbf{G}_a}e^{i\mathbf{G}_a\cdot\mathbf{r}} , \tag{14}$$

where the $\mathbf{G}_a$ are the adsorbate reciprocal-lattice vectors. Therefore, the extrinsic contribution to the free-energy density, namely

$$f_{\text{ext}}\equiv\frac{1}{A}\int d\mathbf{r}\rho(\mathbf{r})V_{\text{ext}}(\mathbf{r}) , \tag{15}$$

where A is the area, can be expressed as

$$f_{\text{ext}}=V(Z_0)\sum_{\mathbf{G}_s}{}^{*}\sum_{\mathbf{G}_a}\rho_{\mathbf{G}_a}\delta(\mathbf{G}_s+\mathbf{G}_a) . \tag{16}$$

Expression (15) reveals all possible adsorbate structures giving $f_{\text{ext}}\neq 0$; i.e., all the possible adsorbate commensurations with the substrate.

The C phases are usually denoted by $C\times C$ with $C=A_a/A_s$, where A_a and A_s are the constants of the adsorbate and substrate lattices respectively. All discussion in this article will focus on a substrate with a triangular lattice. It is straightforward to show that for triangular lattices the δ condition in (16) is equivalent to imposing the relation

$$C=\frac{A_a}{A_s}=(\eta_1^2+\eta_2^2+\eta_1\eta_2)^{1/2} , \tag{17}$$

with $\eta_1=0,1,2,\ldots$ and $\eta_2=1,2,3\ldots$. As the adsorbate mean density must be proportional to A_a^{-2}, only the commensurations with $C=1$, $\sqrt{3}$ and 2 are inside of the physical range of interest. Moreover, the corresponding densities are enough separated each from other that usually there exists only one C phase if any; this is what in fact happens for noble gases on graphite.

IV. THE PARAMETRIZED DENSITY

To describe the particle distribution we use a superposition of Gaussians centered at the adsorbate lattice sites $\mathbf{R}$:

$$\rho(\mathbf{r})=K\sum_{\mathbf{R}} e^{-\alpha(\mathbf{r}-\mathbf{R})^2} , \tag{18}$$

where K is a normalization constant which depends on the mean density and $1/\alpha$ is the width of the Gaussian peaks. With (18) we can describe strong structured densities while the Fourier expansion of $\rho(\mathbf{r})$, (14), is limited to relative smooth densities because of the small number of Fourier components which can be used in practice.

The cumbersome algebra induced by the Gaussians is the price paid for having a good representation of the density $\rho(\mathbf{r})$. The Gaussians will describe not only the crystal but also the fluid. Depending on the phase type the normalization constant K is determined in a different way. The density of a fluid phase is constant ($\alpha=0$) but it can be moderately modulated ($\alpha\neq 0$ but relatively small) by the effect of an external field. In any case, the normalization constant K in a fluid phase is exclusively determined by the total number of particles; then if ρ_0 is the mean density

$$\rho_0=\frac{N}{A}=\frac{1}{A}\int d\mathbf{r}\rho(\mathbf{r})=\frac{K_F\pi}{\alpha C_s} \tag{19}$$

or

$$K_F=\frac{\alpha\rho_0 C_s}{\pi} . \tag{20}$$

C_s being the unit-cell area of the substrate lattice. The fluid phase follows the topology of the substrate and therefore it has the same lattice parameter $A_a=A_s$ which does not depend on the mean density, though the adsorbate density modulation intensity does it. At high densities the adsorbate particles are confined by their neighbors and the system becomes ordered by itself; in this case each site of the adsorbate lattice has a particle, therefore

$$\rho_0=\frac{1}{C_a} , \tag{21}$$

C_a being the unit-cell area of the ordered adsorbate lattice, and

$$1=\frac{1}{C_a}\int_{C_a} d\mathbf{r}\rho(\mathbf{r})=K\pi/\alpha\ , \tag{22}$$

i.e.,

$$K=\pi/\alpha\ . \tag{23}$$

The adsorbate lattice constant A_a will now depend on the mean density through the expression (21) which for a triangular lattice becomes

$$A_a^2=2/\rho_0\sqrt{3}\ . \tag{24}$$

The presence of an external field would modulate the intrinsic ordered phases and eventually change its intrinsic order towards any of the possible extrinsic (commensurate) orders, however this requires the presence of defects (interstitials and vacancies) and domains whose effects will be discussed later. For the moment we restrict ourselves to the effects of the pure competition between the hard-core adsorbate and adsorbate-substrate interactions and entropy disorder, without allowing any relaxation mechanism such as those mentioned.

It could be, however, that at a certain density the order of the I phase would correspond to any of the possible commensurations; then the normalization constant is evaluated in the same way as in the intrinsic ordered case.

Finally, the width constant α is determined by the minimization of the Helmholtz free energy; the details of this are given in Sec. V.

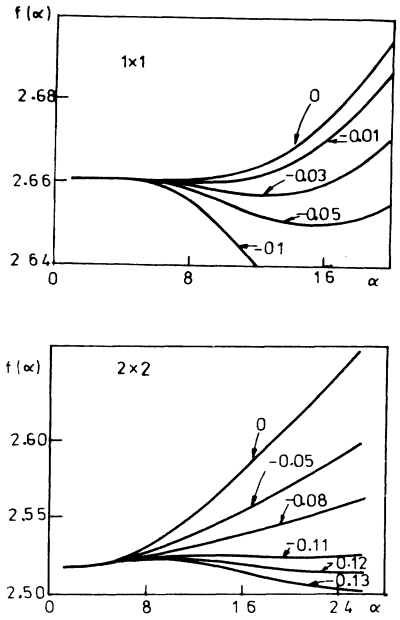

FIG. 1. Upper: free-energy density versus α for the fluid phase and for several values of V^*. $A_s=0.6045d$ and $\rho=0.79/d^2$. Lower: free-energy density versus α for 2×1 C phase for several values of V^*. $A_s=0.61d$; $\rho_{2\times1}=0.7758/d^2$.

V. MINIMIZATION PROCESS

Using the parametrized density (18) we minimize the Helmholtz free-energy functional (1) including the extrinsic contribution (15) and with the help of the weight function (7). The minimization process is done for both ordered and disordered phases at different values of the dimensionless variables $\rho^*=\rho/d^2$ and $V^*=V(Z_0)/k_BT$. Notice that, although the adsorbate is a hard-disk system, the adsorbate-substrate interaction precludes any attempt at temperature scaling.

A. Free-energy branch for the fluid phase

Figure 1 shows the characteristic behavior of the free-energy density of the fluid versus α at $\rho=0.79/d^2$ for $A_s=0.6045d$ and for several values of the parameter V^*. For the zero-field case the minimum occurs at $\alpha=0$ as it should, i.e., the fluid has a homogeneous density distribution; as the external field increases from zero, the fluid density becomes modulated and the minimum free energy corresponds to a slowly increasing α. The fluid density follows the structure of the external field, only in this sense it can be called a 1×1 commensurate phase. $f(\alpha)$ increases with the mean density, though the characteristic behavior of f as a function of α and V^* is similar at different mean densities.

B. Free-energy branch for the intrinsic ordered phase (I phase)

Consider, first, the two-dimensional system of hard disks in the absence of any external potential. The free energy will scale with the temperature, so that we only have to consider the density dependence. At low density the system will be fluid with a homogeneous particle distribution, $\rho(\mathbf{r})=\rho_0$, which means that in our Gaussian parametrization (18) and (23) the free energy as a function of the Gaussian width, $f(\alpha)$, will have a single minimum at $\alpha=0$. However, at larger values of the mean density, the free-energy $f(\alpha)$ will develop a second minimum for $\alpha\neq0$, which represents the intrinsic ordered phase, that is, the adsorbate crystal. This phase starts as a metastable state (Fig. 1), i.e., with larger free energy that the $\alpha=0$ fluid, but at higher mean density becomes the stable phase (see Ref. 9 for details). Now, if we turn on the substrate potential, the fluid will develop a structure, $\rho(\mathbf{r})\neq\rho_0$, with the periodicity of the substrate as described above. The modulation in $\rho(\mathbf{r})$ may be weak or strong depending on the relative size of the adsorbate and the substrate, but there will always be a qualitative change from the homogeneous density distribution to the periodic structure described by (18) and (20).

The other phase, the crystal, is much more difficult to distort than the fluid and it has its own periodicity, which, in general, would not be commensurate with the substrate. Then, as a first approximation, we may neglect any reaction of the system to the external potential and there would be no change in its free energy, because the $\delta(\mathbf{G}_a-\mathbf{G}_s)$ in (16) will vanish. Of course, if the external field produced by the substrate is large compared with the compressibility of the crystal, the intrinsic ordered phase will be distorted. To compromise between the two terms we will include this contribution later but, for the moment we neglect it, so that the free energy of the intrinsic or-

dered phase is taken as the corresponding to the perfect crystal in absence of any substrate modulation.

C. Free energy of the C phase

The lattice parameter of the adsorbate is a function of its mean density (24), so that a continuous change of ρ will eventually produce an intrinsic lattice commensurate with the substrate. Because of the narrow range of density for the crystal phase, one may expect only a few (and usually only one) possible commensurations for a given ratio of the adsorbate and substrate sizes. For these particular values of the mean density, which we will call generically ρ_c, the external potential contributes to the free energy even if the density distribution is not distorted from the intrinsic crystal. This will pull down a point out of the free energy of the crystal by an amount proportional to V. Depending on the value of ρ_c, this commensurate phase will compete with the intrinsic crystal or with the modulated fluid. In the first case the C phase will always be stable because its free energy is always lower than the crystal at the same density. In the second case, a minimum value of $|V^*|$ will be required to stabilize the C phase in the fluid range of density, and only for an even larger $|V^*|$ will it become the stable phase.

At this stage the C phase only exists for a given value of the density, ρ_c, and the system may still remain in this phase by creation of lattice defects. A C phase with a few vacancies will have a mean density lower than ρ_c, while interstitials will increase it. The effect of these relaxation mechanisms will be discussed in the second part of this work.

VI. PHASE DIAGRAM

Figure 2 shows the qualitative example of the behavior of the different free-energy branches discussed in Sec. V. The figure illustrates how the tangent method determines the different phase transitions which we always find to be first order. Notice that the C phase is located at a precise mean density ρ_c.

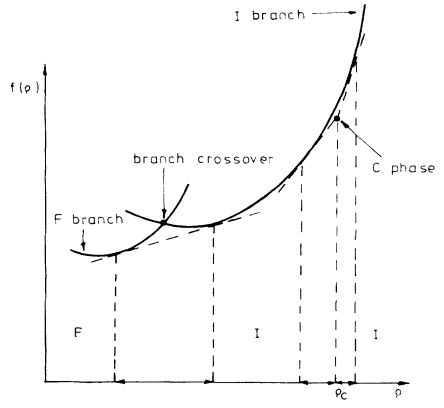

FIG. 2. Qualitative behavior of the free-energy branches at an arbitrary value of V^* and A_s. First-order fluid C, IC, and CI transitions are shown. ρ_c is the C density; Arrows represent density coexistence gaps.

In Fig. 3 we present a sequence of the phase diagrams, in $(\rho d^2, V/k_BT)$ space, obtained with different values of the substrate lattice parameter A_s, in the small range from 0.61 to 0.59 in units of the hard-disk diameter d. Notice that different scales have been used to show the relevant details in each case. The two extremes [Figs. 3(a) and 3(e)] have been obtained with the full Gaussian description described in the preceding sections; but, to save computing effort, the intermediate cases [Figs. 3(b)–3(d)] were calculated with the density expansion of the free-energy functional and by using the Fourier description (14) $\rho(\mathbf{r})$ (see Appendix A). In order to describe simultaneously two phases it is necessary to expand the free-

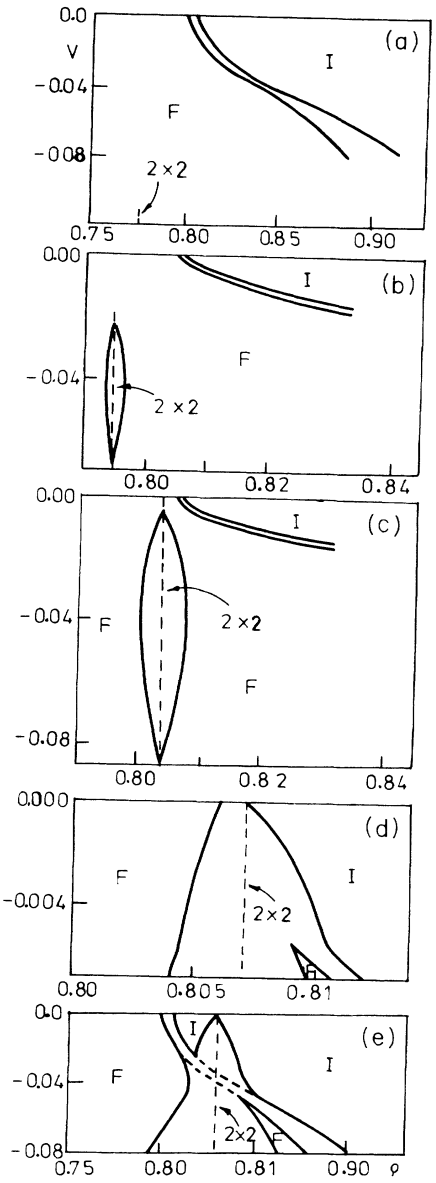

FIG. 3. Phase diagram of hard-disk system under the effect of an external field. From (a) to (e) the triangular lattice parameter is $A_s = 0.610$, 0.603, 0.599, 0.598, and $0.590d$, respectively.

energy functional at least up to fourth order. On the other hand for a given substrate (A_s^*), the Fourier components we must include are $\mathbf{q}^{(1)}$, the first vector of the 2×2 reciprocal lattice to describe the 2×2 C phase and $\mathbf{q}^{(3)}$, the first vector of the 1×1 reciprocal lattice to describe the fluid phase. The 1×1 reciprocal lattice is a sublattice of the 2×2 one, being $|\mathbf{q}^{(3)}|=2|\mathbf{q}^{(1)}|$; therefore, for consistence the intermediate vector $|\mathbf{q}^{(2)}|=\sqrt{3}|\mathbf{q}^{(1)}|$ of the 2×2 reciprocal lattice should also be included. Using the expressions of the Appendix and after simple but cumbersome algebraic steps one arrives at three coupled equations for Fourier coefficients whose solutions give place to the intermediate diagrams (b), (c), and (d) of Fig. 3.

At $V^*=0$ all the diagrams reduce to the plain hard-disk system, which in this theory has a very weak first-order transition[13] from fluid for $\rho\lesssim0.80147d^{-2}$ to a crystal for $\rho\geq0.80592d^{-2}$. The use of the Fourier expansion in the evaluation of the intermediate cases modify the coexisting densities, reducing even more the density gap, $\rho_F=0.80615d^{-2}$ and $\rho_s=0.80700d^{-2}$. As V^* decreases from zero, the fluid phase starts developing the structure with the periodicity of the substrate so that its free energy is lowered, while the crystal forms the I-phase branch which remains unmodified, as we have discussed above. Thus, the fluid phase becomes stable at higher values of the mean density ρ and the fluid to the I-phase transition moves towards larger ρ. Moreover, it is clear in Fig. 3(a), that as the transition is driven towards the right, the density gap between the fluid and the intrinsic crystal gets larger, that is, it has a stronger first-order character. This is a sensible result because at high density the crystal increases rapidly its structure and becomes more rigid, so that the difference with the fluid is stronger.

Now with respect to the C phases, the values used for A_s/d give a 2×2 C phase in the range from $0.775d^{-2}$ to $0.829d^{-2}$, while a $\sqrt{3}\times\sqrt{3}$ occurs for $\rho>1$, well inside the I phase and not far from the close-packing limit. Any other possible commensurations lie at too low a density in the fluid range to be stabilized by any reasonable substrate potential.

For $A_s/d=0.61$ [Fig. 3(a)] the C-phase density is $\rho_c=0.7758d^{-2}$, in the fluid range, so that it is not stabilized until the substrate potential becomes strong enough, $V^*<-0.11$, and even then it is only a metastable phase with respect to the fluid. So in this case, and for physical values of ρ and V^*, the phase diagram is divided between the fluid and the I phase. For the next value of $A_s/d=0.603$ [Fig. 3(b)] we have $\rho_c=0.7939d^{-2}$, still in the fluid side, but this small change is enough to produce a stable C phase for $V^*<-0.025$ with a first-order phase transition from the fluid at low ρ to the C phase and other transition back to a reentrant fluid at higher density.

The coexistence density gaps of these transitions increase with $|V^*|$, but if the field becomes too strong the transition becomes weaker and finally disappears for $V^*\leq-0.07$, where the fluid phase becomes again the stable phase. This may be understood in the sense that for very strong fields the particles are confined very close to the potentials wells, so that our continuous model becomes equivalent to a lattice model, which in this case will present a fluid phase up to the $\sqrt{3}\times\sqrt{3}$ ordering.

In Fig. 3(c) we present the phase diagram for $A_s/d=0.59928$, which takes the C-phase density to $\rho_c=0.8038d^{-2}$, just below the freezing density in absence of external potential. In this case the transition to the C phase appears at lower V^* (higher temperature) and the density gap in the phase transition from the fluid to the C phase is larger. The next case [Fig. 3(d)] corresponds to $A_s/d=0.598$, only 0.2% lower than the preceding one, but this difference brings the C-phase density into the fluid to crystal density gap at $V^*=0$. This fact changes completely the phase diagram. At any $V^*<0$ the fluid-to-I phase transition is split by the C phase, so that there is a fluid-to-C phase transition and then a C-phase to I-phase one, with no reentrant fluid.

Only when the substrate potential becomes stronger and displaces the fluid-to-I phase transition to large ρ, out of the density gap associated to the C phase, it appears again as a reentrant fluid. At this point there is a triple coexistence between the C phase, the I phase, and the reentrant fluid.

Finally, for $A_s/d=0.59$ [Fig. 3(e)] the C-phase density, is $\rho_c=0.829d^{-2}$, in the crystal side at $V^*=0$. In this case at low $|V^*|$ the freezing from fluid to I phase is preserved and only at large ρ the C phase competes with the I phase. As we discussed above, in this situation the C phase is stable for any $V^*<0$, but the density gaps on both sides of ρ_c decreases as $|V^*|$ goes to zero. For larger $|V^*|$ this density gap takes over the fluid to I-phase transition. This happens first at the fluid side with a triple coexistence point between fluid, I phase and C phase, at even larger $|V^*|$. The diagram is similar to the preceding case, with the C phase in between the fluid and the I phase until the other triple point, on the opposite side, gives back the reentrant fluid.

VII. CONCLUSION

We have followed a new approach to the study of adsorbed monolayers based on density-functional formalism. The main difference between this and any previous attempts at a continuous description of the density distribution is that our density-functional model for the free energy of hard disks contains the possibility of a crystal phase at large packing fraction. Thus, we can follow the competition between the intrinsic ordering of the adsorbate and the external potential created by the substrate. To clarify this point in a simple model, before any attempt to get quantitative agreement with real experiments, we have not included at this stage the attractive interactions between adsorbate molecules, which will eventually lead to a gas-liquid condensation in the monolayer.

By using only hard-disk interactions between the adsorbate molecules we make them independent of the temperature, while the smooth substrate potential, V, is scaled with T. Thus the T and V dependence of the phase diagrams reduce to $V^*=V/k_BT$. This is the opposite limit of what can be described in lattice models which would represent infinitely attractive interactions with the substrate which would pin the adsorbate to the lattice sites independently of T. If infinitely repulsive interactions be-

tween the adsorbate are assumed, as in the hard-hexagons model,[8] the system is temperature independent. To get T dependence one has to include finite interactions between the adsorbate molecules, as in the Potts model,[17] so that they are scaled by the temperature. In fact, realistic models for the interactions give rather smooth substrate-adsorbate potentials, while the repulsion between close adsorbate molecules, neglecting attractive interactions, may be fairly described by hard cores. Thus, the real density distribution is going to look more like a smooth profile, and the role of the temperature will be more accurately described by a continuous model.

The second main advantage of our treatment is to have a good description of the crystalline phase for the adsorbate, with a lattice parameter which changes with the pressure, in a range of density from the freezing value to the close-packing limit. The description of this phase with perfect, but incommensurate with the substrate, ordering is not possible in lattice models, which may only refer to the incommensurate phase as the close-packed density of lattice-domain walls,[17] i.e., a situation in which the system is doing its best to break with the substrate ordering but not been able to generate its own.

The results obtained in our calculations show the extreme variety and richness of the phase diagrams, even before the adsorbate-adsorbate attractions add the gas-liquid condensation to the phase diagram. Notice that a variation of only 3% in the ratio between the substrate lattice size and the hard-disk diameter takes the phase diagram from the upper to lower portions of Fig. 3. The evaluation of the free energy of each phase as a function of ρ and T, allows us to appreciate the extreme weakness of the phase transitions. The free-energy differences in Fig. 2 have been grossly exaggerated to make them more visible, as the actual, small differences make the full diagram quite "soft" with respect to any perturbation. In this respect, we have to realize that so far we have considered only states with perfect ordering without any kind of lattice defects. On one hand, this reduces any C phase to a single line at fixed density ρ_c in the (ρ, V^*) phase diagram, though because of the coexistence density gap, the C phase will be present in the system (sharing the monolayer with the other coexisting phase) at mean densities inside that gap. The presence of vacancies and interstitials would make the C phase stable in a finite range of density around ρ_c.

The other problem of the perfect lattice description is that the intrinsic ordered phase, i.e., the adsorbate crystal, is unaffected by the substrate potential. As we have commented this should be a fairly good approximation for high-temperature or smooth substrate potentials, but it will fail if the potential is strong enough. To consider these interactions one should allow the adsorbate crystal to relax its lattice structure to accomodate the particles closer to the substrate wells. If the intrinsic lattice parameter is not too different from one of the commensurated phases, the relaxation process will likely create domain walls between different pieces of the C phase, which occupied different sublattices of the substrate.

Due to the small differences in the free energy of the phases observed here, it is necessary to include these two relaxation processes, before any attempt to quantitative comparison with the experiment. This is done in the second part of this work. However, for the hard-disk system, and in a future publication, we will include the attractive interactions in the adsorbate to examine the interplay between the gas-liquid condensation and the ordering transitions studied here.

ACKNOWLEDGMENTS

The authors wish to thank to Dr. E. Chacón, Dr. R. Evans, Dr. M. Telo da Gamma, Professor M. Fisher, and Professor K. Gubbins for helpful discussions. This work has been supported by the Comision Asesora de Investigaciones Científica y Técnica of Spain and the USA-Spain joint committee for Scientific and Technical Cooperation (Project No. CCB8504023).

APPENDIX

The density expansion of the Helmholtz free energy around a constant density ρ_0 is

$$F[\rho(\mathbf{r})]=F[\rho_0]+\int d\mathbf{r}\left.\frac{\delta F[\rho]}{\delta\rho(\mathbf{r})}\right|_{\rho_0}\Delta\rho(\mathbf{r})+\frac{1}{2}\int d\mathbf{r}\,d\mathbf{r}'\left.\frac{\delta^2 F[\rho]}{\delta\rho(\mathbf{r})\delta\rho(\mathbf{r}')}\right|_{\rho_0}\Delta\rho(\mathbf{r})\,\Delta\rho(\mathbf{r}')+\cdots\,, \tag{A1}$$

where $\Delta\rho(\mathbf{r})$ is the departure from the constant density ρ_0. Using the functional (1) together with the weight function (7), the succesive correlation functions or functional derivatives appearing in (1) are

$$\left.\frac{\delta F[\rho]}{\delta\rho(\mathbf{r})}\right|_{\rho_0}=\mu(\rho_0)\,, \tag{A2}$$

and for $n>1$

$$\begin{aligned}C^{(n)}(\{r^{(n)}\};\rho_0)&\equiv\frac{1}{k_BT}\frac{\delta^{(n)}F[\rho]}{\delta\rho(\mathbf{r}^{(1)})\cdots\delta\rho(\mathbf{r}^{(n)})}\\&=(-1)^n\frac{(n-2)\delta(\mathbf{r}-\mathbf{r}^{(1)})\cdots\delta(\mathbf{r}-\mathbf{r}^{(n)})}{\rho_0^{n-3}}\\&\quad+\frac{\Delta\psi^{(n-1)}}{k_BT}\pi d^2\sum_{i=1}^{n}\omega(|\mathbf{r}^{(i)}-\mathbf{r}^{(1)}|)\cdots\omega(|\mathbf{r}^{(i)}-\mathbf{r}^{(n)}|)+\frac{\rho_0\Delta\psi^{(n)}}{k_BT}\int d\mathbf{r}\omega(|\mathbf{r}-\mathbf{r}^{(1)}|)\cdots\omega(|\mathbf{r}-\mathbf{r}^{(n)}|)\,,\end{aligned} \tag{A3}$$

where $\Delta\psi^{(n)}$ is the nth derivative with respect to ρ_0. For periodic densities we can write

$$\Delta\rho(\mathbf{r})=\sum_{q\neq 0}\Delta\tilde{\rho}(\mathbf{q})e^{i\mathbf{q}\cdot\mathbf{r}}\ . \tag{A4}$$

Using (A3) and (A4) into (A1) we get the Helmholtz free-energy density

$$f[\rho]\equiv\frac{F[\rho]}{A}=f_{id}[\rho_0]+\tfrac{1}{2}\sum_{\mathbf{q}}\tilde{C}^{(2)}(\mathbf{q};\rho_0)\Delta\tilde{\rho}(\mathbf{q})^2 + \sum_{n=3}\left[\frac{1}{n!}\sum_{q^{(1)}}\cdots\sum_{\mathbf{q}^{(n)}}\tilde{C}^{(n)}(\{\mathbf{q}^{(n)}\};\rho_0)\Delta\tilde{\rho}(\mathbf{q}^{(1)})\cdots\Delta\tilde{\rho}(\mathbf{q}^{(n)})\delta(\mathbf{q}^{(1)}+\cdots+\mathbf{q}^{(n)})\right], \tag{A5}$$

where the Fourier transform of the correlation functions are

$$\tilde{C}^{(2)}(\mathbf{q};\rho_0)=\frac{1}{\rho_0}+\frac{2\Delta\psi^{(1)}}{k_BT}\tilde{\omega}(\mathbf{q})+\frac{\rho_0\Delta\psi^{(2)}}{k_BT}\tilde{\omega}(\mathbf{q})^2$$

and

$$\tilde{C}^{(n)}(\{\mathbf{q}^{(n)}\};\rho_0)=\frac{n-2}{\rho_0^{n-2}}+\frac{\Delta\psi^{(n-1)}}{k_BT}\left[\sum_{i=1}^{n}\frac{\tilde{\omega}(\mathbf{q}^{(1)})\cdots\tilde{\omega}(\mathbf{q}^{(n)})}{\tilde{\omega}(\mathbf{q}^{(i)})}\right]+\frac{\rho_0\Delta\psi^{(n)}}{k_BT}\tilde{\omega}(\mathbf{q}^{(1)})\cdots\tilde{\omega}(\mathbf{q}^{(n)})\ ,$$

and $\tilde{\omega}(\mathbf{q})$ is the Fourier transform of the weight function.

[1]F. C. Franck and J. H. van der Merwe, Proc. R. Soc. London **198**, 205 (1949); S. C. Ying, Phys. Rev. B **3**, 4160 (1971); P. Bak, D. Mukamel, J. Villain, and K. Wentowska, *ibid.* **19**, 1610 (1979); V. L. Pokrovski and A. L. Talapov, Phys. Rev. Lett. **42**, 65 (1979).

[2]D. A. Huse and M. E. Fisher, Phys. Rev. B **29**, 259 (1984); S. Ostlund and A. N. Berker, *ibid.* **21**, 5410 (1980).

[3]D. K. Fairobent, W. F. Saam, and L. H. Sander, Phys. Rev. B **26**, 179 (1982); L. M. Sander and J. Hautman, *ibid.* **29**, 2171 (1984).

[4]B. Schaub and D. Mukamel, Phys. Rev. B **32**, 6385 (1985); K. J. Niskanen, *ibid.* **33**, 1830 (1986).

[5]R. J. Gooding, B. Joos, and B. Bergersen, Phys. Rev. B **27**, 7669 (1983).

[6]A. Thomy and X. Duval, J. Chem. Phys. **66**, 1966 (1969), see also, J. Chem. Phys. **67**, 286 (1970); **67**, 1101 (1970); Y. Larher and A Terlain, *ibid.* **72**, 1052 (1980); M. D. Chinn and S. C. Fain, Jr., Phys. Rev. Lett. **39**, 146 (1977); M. Nielsen, J. Als-Nielsen, J. Bohr, and J. P. McTagre, *ibid.* **47**, 582 (1981).

[7]F. E. Hanson, M. J. Maudell, and J. P. McTague, J. Phys. (Paris) Colloq. **38**, C4-76 (1977); F. E. Hanson and J. P. McTague, J. Chem. Phys. **72**, 6363 (1980).

[8]R. J. Baxter, *Exactly Solved Models in Statistical Mechanics,* (Academic, London, 1982), p. 402.

[9]W. A. Steele, Surf. Sci. **36**, 317 (1973).

[10]J. S. Rowlinson and B. Widom, *Molecular Theory of Capillarity* (Oxford University Press, New York, 1982).

[11]S. Nordholm, M. Johnson, and B. C. Freasier, Aust. J. Chem. **33**, 2139 (1980).

[12]P. Tarazona and R. Evans, Mol. Phys. **52**, 847 (1984).

[13]P. Tarazona, Mol. Phys. **52**, 81 (1984).

[14]E. Helfard, H. L. Frisch, and J. L. Lebowitz, J. Chem. Phys. **34**, 1037 (1961).

[15]P. Tarazona, Phys. Rev. A **31**, 2672 (1985).

[16]R. Evans, Adv. Phys. **28**, 143 (1979).

[17]R. G. Caflisch, A. Nihat Berker, and M. Kardar, Phys. Rev. B **31**, 4527 (1985).